

# Traditional Classification Neural Networks are Good Generators: They are Competitive with DDPMs and GANs

Guangrun Wang<sup>1</sup> Philip H.S. Torr<sup>1</sup>

<sup>1</sup> University of Oxford

{guangrun.wang, philip.torr}@eng.ox.ac.uk

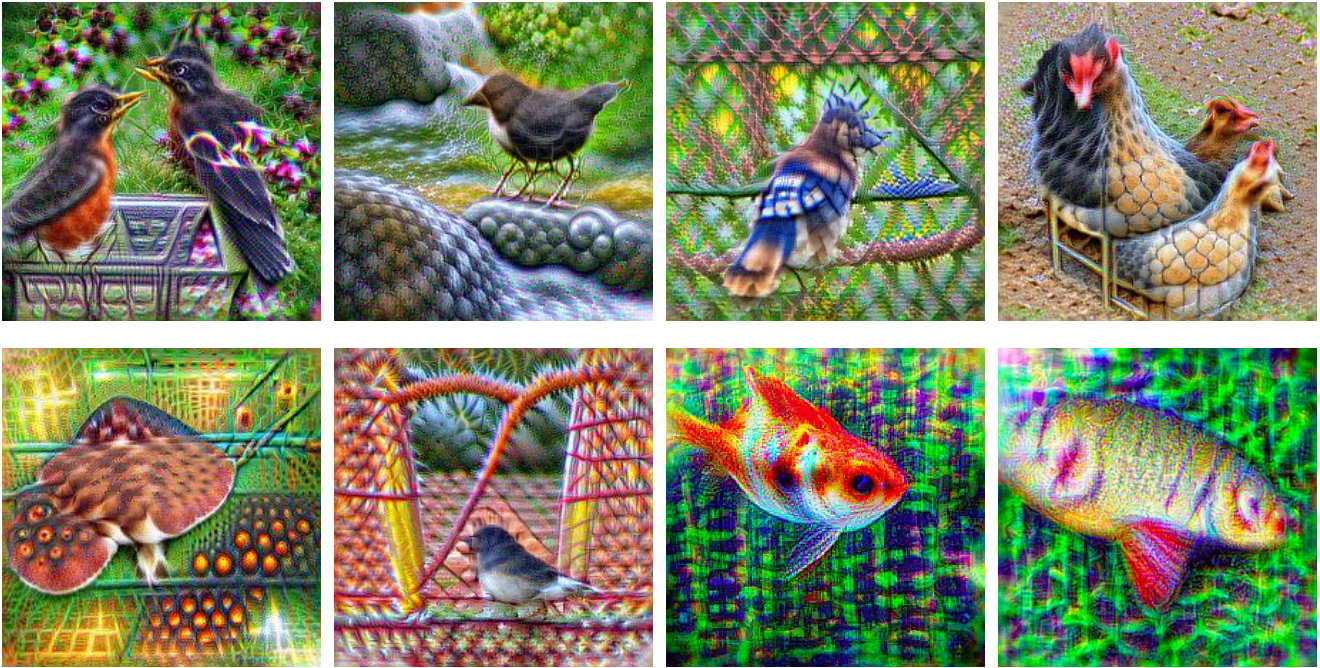


Figure 1. Selected samples generated by classification neural networks on the ImageNet  $256 \times 256$  task (More samples are in the appendix.).

## Abstract

Classifiers and generators have long been separated. We break down this separation and showcase that conventional neural network classifiers can generate high-quality images of a large number of categories, being comparable to the state-of-the-art generative models (e.g., DDPMs and GANs). We achieve this by computing the partial derivative of the classification loss function with respect to the input to optimize the input to produce an image. Since it is widely known that directly optimizing the inputs is similar to targeted adversarial attacks incapable of generating human-meaningful images, we propose a mask-based stochastic reconstruction module to make the gradients semantic-aware to synthesize plausible images. We further propose a progressive-resolution technique to guarantee fidelity, which produces photorealistic images. Furthermore, we introduce a distance metric loss and a non-trivial distri-

bution loss to ensure classification neural networks can synthesize diverse and high-fidelity images. Using traditional neural network classifiers, we can generate good-quality images of  $256 \times 256$  resolution on ImageNet. Intriguingly, our method is also applicable to text-to-image generation by regarding image-text foundation models as generalized classifiers.

Proving that classifiers have learned the data distribution and are ready for image generation has far-reaching implications, for classifiers are much easier to train than generative models like DDPMs and GANs. We don't even need to train classification models because tons of public ones are available for download. Also, this holds great potential for the interpretability and robustness of classifiers. Project page is at <https://classifier-as-generator.github.io/>.

## 1. Introduction

Neural network classifiers [10, 17, 21, 22, 46] have gained remarkable progress in computer vision and machine learning. They achieve human-level performance in many tasks.

Lagging behind neural network classifiers are neural network generators. Over the past few years, neural network generators have made some progress, e.g., in generating texts [3], images [37, 38, 40, 42], sounds [8, 32], videos [47, 55, 59], lights [6, 57], and 3D scenes [4, 5]. Despite that, they are still inferior to neural network classifiers. On the one hand, neural network classifiers are easier to learn than generators in terms of efficiency and stability. For example, training a classification net is straightforward; but training a GAN [13] could easily lead to model collapse and non-convergence, and training a DDPM [9, 19, 30] requires complicated efforts. On the other hand, neural network classifiers can better model the data’s true distribution than generators. Specifically, classifiers can project the data into the correct latent space so that objects can be reasonably distributed in the latent space according to the category they belong to; in contrast, the mapping between the latent space and the data space for GANs and DDPMs is chaotic, i.e., their latent codes contain less semantic signals, especially for DDPMs. As a typical consequence, the features learned by neural network generators are often less generalizable and transferrable than classifiers.

Since neural network classifiers are so knowledgeable and data-distribution-aware, we ask: are they ready for image generation? It is widely known that directly optimizing the inputs of neural network classifiers does not produce human-meaningful images, for it is equivalent to a targeted adversarial attack. Given this, prior arts utilize multiple regularization methods to help visualize the features of neural networks, e.g., via frequency penalization [23, 24, 29, 33, 34, 54], transformation invariance [7, 24, 25, 31, 33, 34, 54], adversarial training [11, 45, 53], and energy-model-based training [15]. However, as tools for feature visualization, while these methods can certainly produce some better visualizations than random noise, there is a considerable gap between their visualizations and realistic images in terms of plausibility, fidelity, and diversity (see Figure 2). **First**, their visualizations unreasonably contain duplicated patterns everywhere (e.g., many copies of dog eyes in an image), which looks quite implausible. **Second**, their visualizations lack fidelity. The produced images are low-quality, looking fake and unnatural. **Third**, their visualizations are severely lacking diversity. Visualizations produced by different random noises share similar content and style. Besides, some method needs well adversarial training that often suffers from robust overfitting and is time-consuming.

In this paper, we showcase that traditional classification neural networks can synthesize high-quality images at

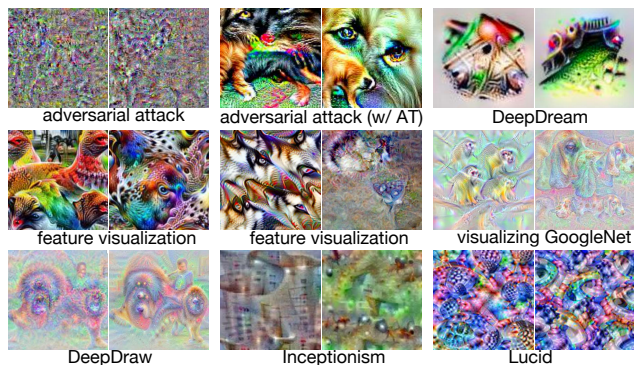


Figure 2. Samples of feature visualization methods. These methods include adversarial attack [14], adversarial robustness as a prior [11], DeepDream [24], feature visualization [7], reproduced feature visualization [11], visualizing GoogleNet [34], DeepDraw [33], Inceptionism [25], and Lucid [11, 31]. Here, AT denotes adversarial training. Note that these samples are from their papers or blogs. Thank the authors.

ImageNet large scale that contains a thousand object categories, being comparable to state-of-the-art generative models (e.g., DDPMs and GANs). To accomplish this, we compute the partial derivatives of the classification loss function with respect to the inputs to optimize the inputs to produce images. But this alone cannot generate plausible, realistic, and diverse images. For **plausibility**, we introduce a mask-based stochastic reconstruction module to make the gradients semantic-aware to generate reasonable images. This module can significantly improve plausibility as well as fidelity. For **fidelity**, we further propose a progressive-resolution generation technique, starting with optimizing  $64 \times 64$  images and ending up with optimizing  $256 \times 256$  images. This technique could reduce diversity as it is widely known that fidelity and diversity have a tradeoff. Finally, to break the curse of compromise between fidelity and **diversity**, we introduce a distance metric loss as well as a nontrivial distribution loss to guarantee the synthesized images are of good diversity.

Intriguingly, our method also applies to text-to-image generation, for we can regard image-text foundation models as generalized classifiers – maximizing the inner product between an image and a text reduces to classifying this image to this text. Our method can use texts to produce meaningful samples.

In summary, this paper makes five contributions.

- We showcase that traditional neural networks can generate high-quality images at ImageNet large scale, competitive with state-of-the-art generative models. This has far-reaching implications since classifiers are easier to obtain than generators; it also holds potential for the interpretability and robustness of classifiers.
- We address the implausibility of directly optimizing



the inputs using a mask-based stochastic reconstruction module to make the gradients semantic-aware to synthesize reasonable images.

- We propose a progressive-resolution generation technique to guarantee fidelity, which is capable of producing photorealistic images.
- To increase diversity, we introduce a distance metric loss and a nontrivial distribution loss to guarantee the diversity of the generated images of the same class.
- Using traditional neural network classifiers, we can generate good-quality samples on the ImageNet  $256 \times 256$  task. Intriguingly, our method can also achieve text-to-image generation via regarding image-text foundation models as generalized classifiers.

## 2. Related Work

**Feature visualization.** Visualizing neural network features has been a long-standing vision [58], where the focus is on understanding neural networks rather than generating images. To produce human-meaningful visualizations, prior works use a variety of regularization methods to make the results somewhat interpretable. These regularization methods include high-frequency penalty [23, 24, 29, 33, 34, 54], transformation invariance [7, 24, 25, 31, 33, 34, 54], adversarial training [11, 45, 53], and energy-model-based training [15]. However, these methods are just limited to visualization for explainability, and the visualizations look fake regarding plausibility, fidelity, and diversity. Classifiers acting as good generators are still absent currently.

**Classifier-guided generative models.** Some work has begun to use classifiers as guidance to control the production of generative models. This involves using a pretrained classifier to optimize the latent space of GANs (often called GAN inversion) [12, 27, 28, 35] and to optimize the sampling direction of DDPMs [9, 48, 51]. While these methods demonstrate the power of classifiers for image generation, they are heavily dependent on existing generators (such as GANs or DDPMs). Unlike these methods, we showcase that traditional neural network classifiers already know the data distribution and are ready for image generation.

**DDPMs.** Although significantly different from DDPMs, our method has some connections to DDPMs [9, 19, 30]. DDPMs are likelihood-based generative models that have been shown to produce high-fidelity images. However, just as Rome wasn’t built in a day, DDPMs are being improved through the joint efforts of many articles [1, 19, 20, 30, 43, 48–51]. While DDPMs have achieved some success, they have some deficiencies over neural network classifiers. First, DDPMs are harder to train than neural network classifiers. Second, the latent space of DDPMs is less semantic than that of neural network classifiers.

## 3. Neural Network Classifier as Generator

In this section, we first review neural network classifiers. Then, we introduce how to convert their learned knowledge into reasonable, high-fidelity, and diverse images from three aspects: plausibility, fidelity, and diversity. Finally, we present the connection between our method and DDPMs, and how to extend it for text-to-image generation. For the sake of brevity, we use CaG to term our method, which is short for “Classifier as Generator.”

### 3.1. Neural Network Classifier

The formulation of neural network classifiers is very simple, and people are quite familiar with it. Let  $f$  denote a neural network,  $x$  its input image, and  $p$  its output logits before softmax normalization. Then a neural network classifier is written as  $p = f(x)$ . The prediction of this classifier is the index in which the value is the largest in  $p$ . More generally, a neural network classifier can be a cross-modal model for a text-to-image modeling task like CLIP [36].

Unlike all generators, neural network classifiers are directly trained independently on classification tasks such as ImageNet or CIFAR-10. Note that training neural network classifiers is much easier than generators. Also, tons of classification models are available for download online, so we don’t even need to train them.

We hope that using the knowledge of the neural network classifier, through step-by-step iterations, we can turn a random input into an expected sample and achieve image generation. Figure 3 (a) shows a framework we envision.

#### 3.1.1 An initial idea for generation

With a trained neural network classifier  $f$  and a given class label  $c$ , one can use a classification loss to encourage the classifier to predict this label. In this way, a generation problem reduces to an optimization problem. Specifically, one can compute the partial derivative of the loss with respect to the input  $x_t$  and optimize  $x_t$  such that the prediction of the neural network classifier is  $c$ :

$$x_{t+1} = x_t - \arg \min_{\Delta x_t} \mathcal{L}_{\text{cls}}(f(x_t + \Delta x_t), c), \quad (1)$$

where  $t$  denotes the time sequence of the optimization.  $\mathcal{L}_{\text{cls}}$  is the classification loss;  $x_0$  is an initial tensor.

Unfortunately, Eqn. (1) is equivalent to a targeted adversarial attack, which is widely known to be unable to generate human-meaningful images. An initial idea for using a neural classifier as a generator is shown in Figure 3 (b).

### 3.2. Mask-Based Stochastic Reconstruction Module

Mathematically, the optimization problem in Eqn. (1) treats the high-dimensional input space as the unknown

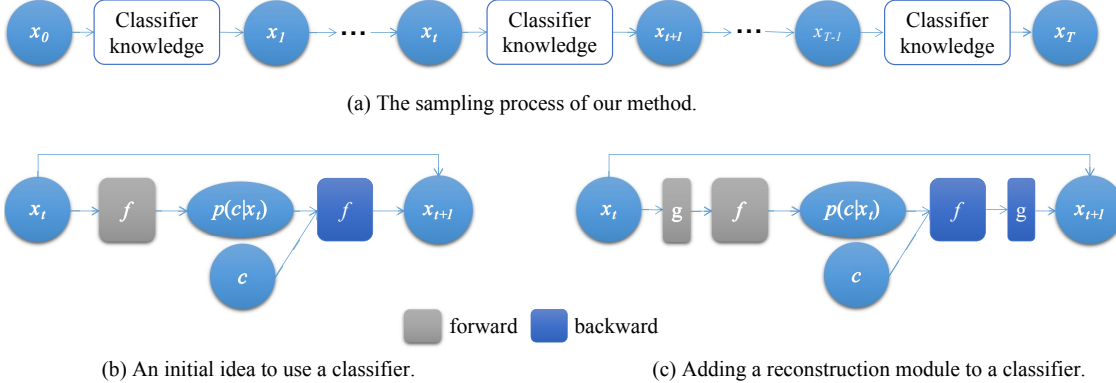


Figure 3. Illustration of our method. (a) is the sampling process of our method, and the key to its success is to exploit the knowledge of the classifier, which can be implemented in two ways, as illustrated in Figures (b) and (c). (b) An initial idea to use a classifier for generation, but the gradients are, unfortunately, semantic-agnostic. (c) By adding a mask-based stochastic reconstruction module to the classifier, the gradients are made semantic-aware to synthesize human-meaningful images.

variable to be solved, which has infinitely many solutions. Many of these solutions are semantic-agnostic.

To address the above dilemma, we propose a mask-based stochastic reconstruction model to make gradients semantic-aware to generate plausible images. Specifically, the gradients may guide the variables to be solved towards a local optimum to satisfy Eqn. (1), resulting in human-meaningless images. Fortunately, [16] and [56] showcase that mask-based stochastic reconstruction models are semantically aware. Inspired by these two papers, we add a mask-based random reconstruction module to the input images:  $x \leftarrow g(x)$ , where  $g$  is a masked auto-encoder [16], defined by:

$$g^* = \min_g \mathbb{E}_{x \sim \mathcal{D}} \|m(g(\bar{m}(x))) - m(x)\|_2^2, \quad (2)$$

where  $\mathbb{E}$  represents the mathematical expectation.  $\mathcal{D}$  represents the data distribution.  $m$  represents an operation that obtains the masked region of an image.  $\bar{m}$  is complementary to  $m$ , meaning a procedure that gets the unmasked part of an image. Hence, Eqn. (1) can be rewritten as:

$$x_{t+1} = x_t - \arg \min_{\Delta x_t} \mathcal{L}_{\text{cls}}(f(g(x_t + \Delta x_t)), c). \quad (3)$$

Here,  $g$  is a general mask-based stochastic reconstruction module that can be pretrained with general images. Many of them are available for download online, so we don't need to train them, either (see the experimental section for detail).

An illustration of a classifier with a mask-based stochastic reconstruction module is presented in Figure 3 (c). We explain why  $g$  can make gradients semantic-aware as follows: in the absence of  $g$ , there are many gradient directions that can make the loss in Eqn (1) drop; but in the presence of  $g$ , many of these gradient directions are invalid because they cannot complete the reconstruction task to reach the final classification goal; in this way, the gradients are regularized to be semantic-aware of the objects to synthesize plausible images.

### 3.3. Progressive-Resolution Generation Technique

Empirically, we find that if the input resolution is larger, the generated images are more diverse but with some minor noise on the image surface. Although these slight noises do not affect humans' recognition of the images, they affect the fidelity of the images. On the contrary, if the input resolution is smaller, the resulting images will be less diverse, but the images will be more realistic.

To guarantee fidelity, we propose a progressive resolution generation technique. We start by producing images of  $64 \times 64$  resolution and gradually increase the resolution of the resulting images exponentially. Specifically, we sequentially generate images of  $64 \times 64$ ,  $128 \times 128$ , and  $256 \times 256$ .

This is definitely different from the traditional super-resolution task<sup>1</sup>; actually, it is a process similar to cognitive imagination. Initially, the overall framework configuration is imagined. The details are then gradually imagined. Through this progressive process, we significantly improve the fidelity of the image.

### 3.4. Distance Metric Loss

On the scalability of our method, we ask: since we can impose a classification loss function to optimize the input to generate reasonable images, can we impose other loss functions to guide reasonable image generation?

In addition to fidelity, diversity is another critical metric for evaluating image generation quality. Therefore, we introduce a diversity-encouraging loss function to verify the scalability of our method, hoping that it will improve the diversity of the generated images. The diversity-encouraging loss function is defined as a distance metric loss:

$$\mathcal{L}_{\text{div}}(x^1, \dots, x^N) = \sum_{\substack{i \neq j; \\ x^i, x^j \in y}} h^T(g(x^i))h(g(x^j)), \quad (4)$$

<sup>1</sup>In fact, our method lacks a super-resolution module commonly used in DDPMs or GANs, which puts our model at an unfair disadvantage.



where  $h$  is the feature extractor in the classifier  $f$  in Eqn. (1), i.e.,  $h$  is the remaining part of  $f$  after removing the last linear layer.  $x^i$  indicates the  $i$ -th generated sample of class  $y$ . Here,  $N$  represents the number of images generated for the same class  $y$ . The meaning of Eqn. (4) is obvious, i.e., we hope the similarity between the images generated for the same class to be small. Combining Eqn. (3) and (4) yields:

$$x_{t+1}^i = x_t^i - \arg \min_{\Delta x_t^i} \left( \mathcal{L}_{\text{cls}}(f(g(x_t^i + \Delta x_t^i)), c) + \mathcal{L}_{\text{div}}(x_t^1, \dots, x_t^i + \Delta x_t^i, \dots, x_t^N) \right). \quad (5)$$

**Remark.** Experimental results show that the distance metric loss can improve the diversity of the generated images, also proving that our method has good scalability because maybe other loss functions for other tasks also work.

### 3.5. Exploiting Distribution Loss

We point out in the Remark of Section 3.4 that, thanks to the scalability of our method, any potential loss function can be introduced to achieve some purpose. In state-of-the-art methods (such as GANs and DDPMs), the distribution of the training set is implicitly exploited. Given that it is reasonable to obtain the data distribution, we feed the data of each class to the neural network classifier, calculate the distribution of its output features, and use these statistics to construct a loss function to guide the generation of samples. Specifically, let the mean of the feature of the  $c$ -th class data be  $\mu_c$  and the variance be  $\sigma_c^2$ , then the distribution loss for generating samples of this class is formulated as:

$$\mathcal{L}_{\text{distribution}}(x^1, \dots, x^N) = (\bar{x}_c - \mu_c)^T (\bar{x}_c - \mu_c) + (S_c - \sigma_c)^T (S_c - \sigma_c), \quad (6)$$

where:

$$\bar{x}_c = \frac{1}{N} \sum_{i=0}^N h(g(x^i)), \quad (7)$$

$$S_c = \frac{1}{N-1} \sum_{i=0}^N (h(g(x^i)) - \bar{x}_c)^2.$$

Introducing this formula can significantly improve the diversity of samples generated by CaG.

**Remark.** Being able to properly optimize the input without introducing adversaries is one of the main properties of our method. This property makes our method highly scalable, opening up many possibilities for future applications.

### 3.6. Sampling

Sampling is the inference phase of a generative model. A good sampling strategy is critical to the sample generation quality. According to the framework of our method introduced above, the role of random masking to CaG is roughly

Table 1. Quantitative comparison between our method and state-of-the-art methods on the ImageNet  $256 \times 256$  task. † indicates a differentiable FID score.

Resolutions	Methods	FID ↓	IS ↑
$256 \times 256$	BigGAN-deep [2]	6.95	
	IDDPM [30]	12.26	
	SR3 [43]	11.30	
	DCTransformer [26]	36.51	
	VQ-VAE-2 [39]	31.11	
	ADM [9] w/o condition, w/ guidance	12.00	95.41
	DeepDream [24]	134.69	22.60
	Ours	6.88 †	326.33

equivalent to Gaussian sampling to GANs and DDPMs, which is indispensable. The sampling process of CaG is detailed in Figure 3 (a), which looks very like the sampling process of DDPM. Specifically, although neural network classifiers and DDPMs are trained in quite different ways, they share some similarities in the sampling phase: they generate images by stepwise sampling, predict the sampling direction, and introduce noise to this direction.

### 3.7. Text-to-Image Generation

CaG can be easily generalized to text-to-image generation tasks. As mentioned in Section 3.1, text-to-image foundation models (e.g., CLIP [36]) can be seen as a generalized classifier. We can extract embeddings for text via the text encoder and combine the text embedding to form the weights of a linear layer, and then impose this linear layer on top of the image encoder. Then, we can get a neural network classifier. After obtaining this neural classifier, we can use Eqn. (3) and either Eqn. (4) or Eqn. (6) to produce realistic samples.

## 4. Results

**Datasets.** To evaluate our method, we conduct experiments on ImageNet at a scale of  $256 \times 256$  resolution. I also experimented with text-to-image generation in the wild.

**Metrics.** We use the FID metric [18] since it measures both the fidelity and diversity of the generated samples. We also use the IS metric [44] that measures how the generated instances are reasonable and how they capture the distribution of the overall dataset. While these metrics are, in many cases, good indicators of the sample quality, they are still problematic. **So we also show a lot of pictures.**

### 4.1. State-of-the-Art Image Synthesis

The table compares CaG with state-of-the-art techniques in Table 1. Our method achieves promising numbers, being comparable to DDPMs and GANs. Note that these comparisons are a bit unfair for our methods. This is because some of the competitors employ super-resolution modules

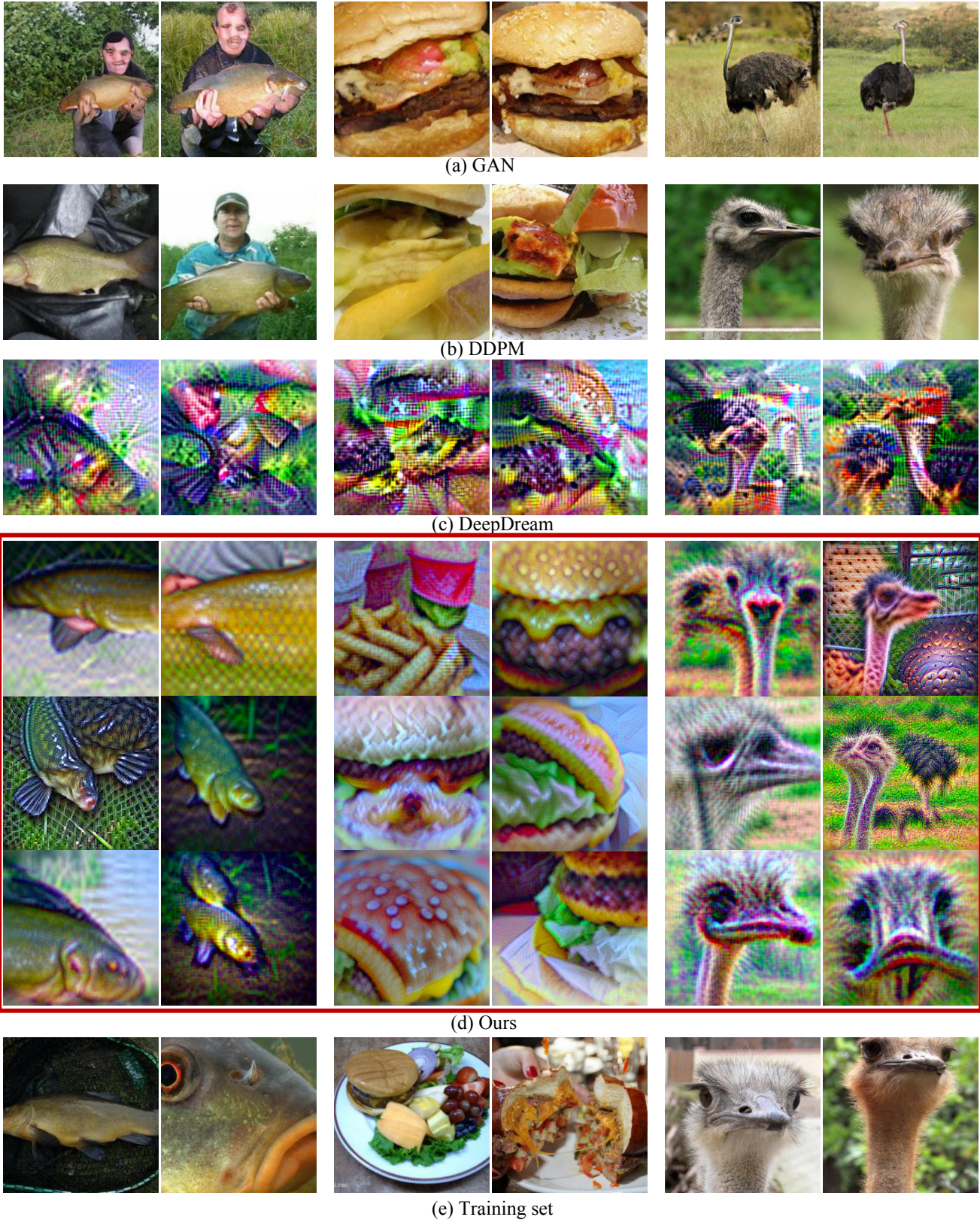


Figure 4. Samples from a GAN (i.e., BigGAN-deep [2]) vs. samples from a DDPM (i.e., ADM [9]) vs. samples from a feature visualization method (i.e., DeepDream [24]) vs. samples from our method and samples from the training set. Note that some of these samples are from their paper. Thanks to the authors. More samples are in the appendix.





Figure 5. Samples of CaG on ImageNet  $256 \times 256$ . The classes are Class 112 (i.e., conch), Class 113 (i.e., snail), Class 113 (i.e., snail), Class 115 (i.e., sea slug), and Class 116 (i.e., chiton). More samples are in the appendix.

that we did not engage in, which is unfair to our method and leaves our approach at an unfair disadvantage position. Regardless, our method achieves good numbers, and it does not require complex training as prior generative models do.

Figure 4 compares randomly selected generated samples

of CaG with that of best-performing methods, including BigGAN-deep [2], ADM [9], and DeepDream [24]. The three represent state-of-the-art GAN, DDPM, and feature visualization algorithms, respectively. In terms of visual effects, all methods have good visual perceptual quality





Figure 6. Samples of CaG on ImageNet  $256 \times 256$ . The classes are Class 117 (i.e., chambered nautilus), Class 118 (i.e., Dungeness crab), Class 120 (i.e., fiddler crab), Class 121 (i.e., king crab), and Class 125 (i.e., hermit crab). More samples are in the appendix.

except DeepDream, which has very poor visual quality. However, our method has stronger semantic perception, resulting in more significant semantic-driven diversity than GANs and DDPMs. **First**, CaG pays more attention to object diversity than background diversity, proving that CaG

is more semantically aware of diversity. For example, in images generated by CaG, birds occupy a large area of the picture. This is consistent with human cognition, for background diversity is easy to achieve by pasting objects to different backgrounds, while object diversity is challenging to





Figure 7. Text-to-image generation using a pretrained text-image model CLIP [36]. Note that we are not chasing high sample quality here, but using fast optimization to get results. We also did not use distance metric loss to increase the diversity of samples. More samples are in the appendix.

obtain. **Second**, CaG decouples and removes irrelevant object categories, generating only the categories we want. For example, CaG’s samples frequently included only individual Tinca fishes that were not held by people, significantly different from the samples of GANs, DDPMs, and even the training set. **Third**, the CaG appears to be aware of geometric information. The images generated by CaG have different orientations, and these orientations include not only the affine transformation of the plane but also different views in the 3D perspective. Finally, CaG is more reasonable, high-fidelity, and diverse than traditional feature visualization methods. Moreover, the CaG algorithm is more robust and reproducible than DeepDream and does not require excessive parameter tuning.

We have provided samples generated by our method in Figure 1 and Figure 4 of the paper. However, the optimization time for each sample needs to be longer, and the number of samples shown needs to be more. Therefore, we present a large number of samples in detail in this supplementary material. Please feel free to review Figures 10, 11, 12, 13, 5, 14, 6, 15, 16, 17, and 18 below in the Appendix.

## 4.2. Text-to-Image Generation

As described in Section 3.7, our method can be used for text-to-image generation straightforwardly. We downloaded the CLIP model [36] and treated CLIP as a generalized classifier, as described earlier. We then use Eqn. (3) for optimization. The results are presented in Figure 7.

Since this is just an extended experiment, we do not pursue the quality of the generated samples, so a quick experiment is performed. Figure 7 shows that our method has great potential for text-to-image generation. Our method can not only understand abstract semantics for image generation (such as “a man loves a woman”) but also generate scenarios that do not exist in reality (such as “a man plays basketball on the moon”), which is very intriguing.

We also compare our method with the state-of-the-art text-to-image generation method DALL.E [38]. As shown in Figure 8, our method generates images with higher fidelity than DALL.E. Be aware that our method is just a generic classifier that is not specifically trained for generative purposes.

In the appendix, we show more examples of text-to-





Ours

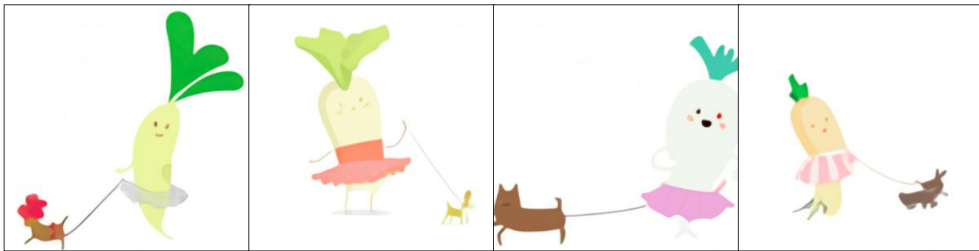


DALL.E

“an armchair in the shape of an avocado”



Ours



DALL.E

“an illustration of a baby daikon radish in a tutu walking a dog”

Figure 8. Text-to-image generation using a pretrained text-image model CLIP [36]. Note that we are not chasing high sample quality here, but using fast optimization to get results. More samples are in the appendix. DALL.E [38] sample are from their blog. Thank the authors.



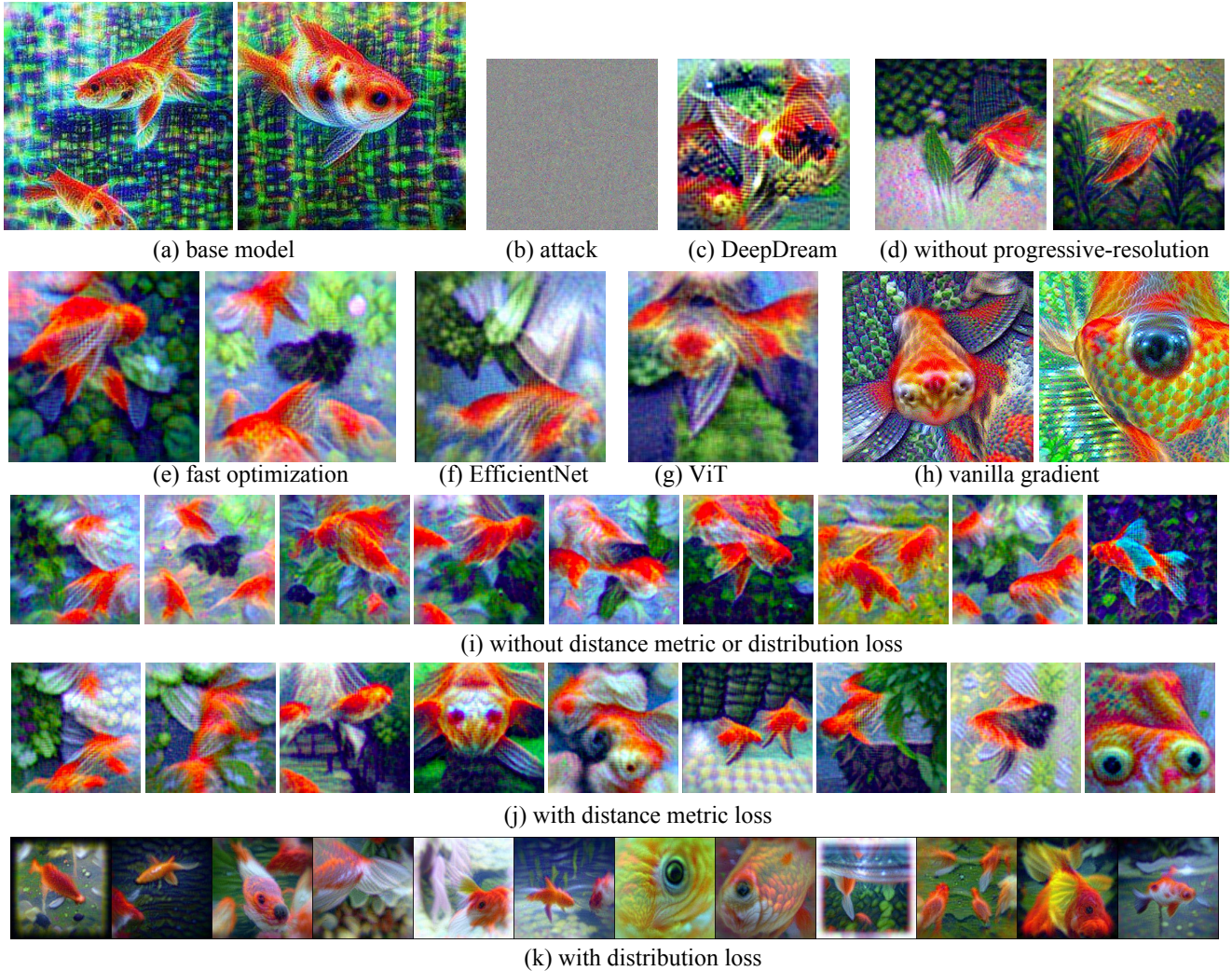


Figure 9. Ablation studies on our method. Note that in order to obtain the results quickly, we use fast optimization (i.e., fewer sampling steps with gradient blurring) except for Figures 9 (a) and (g). Therefore, the resolution of each image is somewhat low.

image generation. Please feel free to review Figures 19, 20, 21, and 22 below in the Appendix.

### 4.3. Ablation Study

In this section, we analyze the components of our algorithm to provide deeper insights.

**Mask-Based Stochastic Reconstruction.** It is widely known that when a target is given, optimizing the input is like a targeted adversarial attack – although the output prediction of the system can be the same as the given target, human-meaningful samples cannot be generated. This is because the partial derivative of the loss function with respect to the input is semantic-agnostic. Here, we examine whether an additional reconstruction module can regularize the partial derivatives to make them semantic-aware to produce human-meaningful images [16, 41, 56]. Figure 9 (a) is the base model, and Figure 9 (b) is a model similar

to Figure 9 (a) but without a mask-based stochastic reconstruction module. The comparison between Figure 9 (a) and (b) showcase this reconstruction module plays a critical role in producing human-meaningful samples.

DeepDream [24] avoids the semantic-agnostic gradient problem by smoothing the gradients with Gaussian blurring. We also compare the mask-based stochastic reconstruction technique with gradient blurring in Figure 9 (a) and (c). The results show that our method yields remarkably better results than gradient blurring. These comparisons prove the indispensability of the stochastic reconstruction module, justifying our conjecture.

**Progressive-Resolution.** Stepwise sample generation from  $64 \times 64$  to  $256 \times 256$  resolution is adopted as our strategy. For comparison, here we remove this progressive resolution strategy, i.e., we directly generate images of the desired resolution. The experimental results are shown in Fig-

ure 9 (d), from which we can see that after removing the progressive resolution strategy, some strange patterns appear in the sample, and the sample fidelity is reduced, which proves the necessity of the progressive resolution strategy.

**Distance metric loss.** Besides classification loss, we also introduce distance metric loss to encourage the diversity of samples. Figure 9 (j) contains distance metric loss while 9 (i) does not contain it. The comparison between Figure 9 (i) and (j) shows that distance metric loss can indeed increase the variety of samples. It produces samples with greater semantic-aware diversity than cross-entropy loss and does not mechanically mimic the training set as cross-entropy loss does. This verifies the effectiveness of the proposed distance metric loss.

**Distribution Loss.** Next, we ablate the distribution loss for the study. By comparing Figures 9 (i) and (k), we can confirm that distribution loss can improve the diversity and fidelity of samples. Further, by comparing Figures 9 (j) and (k), we can know that the effects of distribution loss and distance metric loss are slightly different.

**Architectural Impact.** Unlike prior generators that required difficult training, we do not need to train any models. Our neural network classifier is downloaded from the internet <sup>2</sup>, and the mask-based stochastic reconstruction module is also downloaded from the internet <sup>3</sup>. Given that so many models are available on the Internet, we are free to choose any architecture for image generation. The comparison between Figure 9 (f) and (g) shows that different architectures generate different samples. Here, without loss of generality, we choose two typical neural network classifier architectures: Inception [52] as the representative of convolutional neural networks [22], and ViT-S [10] as the representative of vision transformers [10]. For simplicity, we choose ViT-B for the mask-based random reconstruction module to save computational costs.

We also try to integrate neural network classifiers of different architectures. Specifically, we optimize an input such that it can reduce the loss of Inception and ViT-S simultaneously. The comparison of Figure 9 (e) vs. (f) and the comparison of Figure 9 (e) vs. (g) show that ensembling can further improve the quality of the generated images. Therefore, in this paper, we use this ensembling setting by default.

**Sampling Steps.** Here, we compare the samples at different sampling steps to determine the relationship between image generation quality and sampling steps. Figure 9 (a) shows that the best generation results are achieved when the sampling step number is about 3000. Most of the time, in order to quickly verify our algorithm, we only sample 2000 times (see “fast optimization” in Figure 9 (e)). Increasing

<sup>2</sup><https://pytorch.org/vision/stable/models.html>; <https://github.com/rwightman/pytorch-image-models>.

<sup>3</sup><https://github.com/facebookresearch/mae>; <https://github.com/open-mmlab/mmselfsup>.

the sampling steps within a certain range will make the effect better. Increasing sampling steps further might result in over-optimization.

**Gradient Blurring.** Prior arts [24] showed that Gaussian blurring of gradients is beneficial to increase their semantic perception. Therefore, we also explored the comparison of adding gradient blurring and not adding gradient blurring. Specifically, gradient blurring refers to filtering the gradients of the three channels separately with Gaussian filters. Comparing Figures 9 (e) and (h), we can find that using gradient blur makes the optimization converge faster, but at the expense of image fidelity. Therefore, in the case of fast optimization, gradient blurring is used by default in this paper. But it must be made clear that in our method, gradient blurring is not required.

## 5. Conclusion

We showcase that traditional classification neural networks have strong image generation capabilities, which were previously overlooked. Proving that classifiers have learned the data distribution and are ready for image generation has far-reaching implications, for classifiers are much easier to train than generative models like DDPMs and GANs. We don’t even need to train classification models because tons of public ones are available for download. Also, this holds great potential for the interpretability and robustness of classifiers. For example, people have wondered what explainable artificial intelligence could look like for years. In particular, efforts are being made to try to build new interpretable neural networks. Given that traditional classification neural networks can be used to generate diverse and high-fidelity samples, they can also be used to produce explanations for their decision-making or their predictions. We conjecture that new neural networks may not be needed because existing neural networks already have sufficient interpretability.

**Broader Impacts and Limitations.** Proving that the neural network classifier can complete the generation task can make classification neural networks more transparent but may also bring some unpredictable and uncontrollable privacy or data leakage problems.

## References

- [1] Anirudh Goyal ALIAS PARTH GOYAL, Nan Rosemary Ke, Surya Ganguli, and Yoshua Bengio. Variational walkback: Learning a transition operator as a stochastic recurrent net. *Advances in Neural Information Processing Systems*, 30, 2017. 3
- [2] Andrew Brock, Jeff Donahue, and Karen Simonyan. Large scale gan training for high fidelity natural image synthesis. *arXiv preprint arXiv:1809.11096*, 2018. 5, 6, 7
- [3] Tom Brown, Benjamin Mann, Nick Ryder, Melanie Subbiah, Jared D Kaplan, Prafulla Dhariwal, Arvind Neelakan-



- tan, Pranav Shyam, Girish Sastry, Amanda Askill, et al. Language models are few-shot learners. *Advances in neural information processing systems*, 33:1877–1901, 2020. 2
- [4] Eric R Chan, Connor Z Lin, Matthew A Chan, Koki Nagano, Boxiao Pan, Shalini De Mello, Orazio Gallo, Leonidas J Guibas, Jonathan Tremblay, Sameh Khamis, et al. Efficient geometry-aware 3d generative adversarial networks. In *Proceedings of the IEEE/CVF Conference on Computer Vision and Pattern Recognition*, pages 16123–16133, 2022. 2
- [5] Eric R Chan, Marco Monteiro, Petr Kellnhofer, Jiajun Wu, and Gordon Wetzstein. pi-gan: Periodic implicit generative adversarial networks for 3d-aware image synthesis. In *Proceedings of the IEEE/CVF conference on computer vision and pattern recognition*, pages 5799–5809, 2021. 2
- [6] Zhaoxi Chen, Guangcong Wang, and Ziwei Liu. Text2light: Zero-shot text-driven hdr panorama generation. *arXiv preprint arXiv:2209.09898*, 2022. 2
- [7] Ludwig Schubert Chris Olah, Alexander Mordvintsev. Feature visualization. In *Distill*, 2017. URL: <https://distill.pub/2017/feature-visualization/>. 2, 3
- [8] Prafulla Dhariwal, Heewoo Jun, Christine Payne, Jong Wook Kim, Alec Radford, and Ilya Sutskever. Jukebox: A generative model for music. *arXiv preprint arXiv:2005.00341*, 2020. 2
- [9] Prafulla Dhariwal and Alexander Nichol. Diffusion models beat gans on image synthesis. *Advances in Neural Information Processing Systems*, 34:8780–8794, 2021. 2, 3, 5, 6, 7
- [10] Alexey Dosovitskiy, Lucas Beyer, Alexander Kolesnikov, Dirk Weissenborn, Xiaohua Zhai, Thomas Unterthiner, Mostafa Dehghani, Matthias Minderer, Georg Heigold, Sylvain Gelly, et al. An image is worth 16x16 words: Transformers for image recognition at scale. *arXiv preprint arXiv:2010.11929*, 2020. 2, 12
- [11] Logan Engstrom, Andrew Ilyas, Shibani Santurkar, Dimitris Tsipras, Brandon Tran, and Aleksander Madry. Adversarial robustness as a prior for learned representations. *arXiv preprint arXiv:1906.00945*, 2019. 2, 3
- [12] Federico A Galatolo, Mario GCA Cimino, and Gigliola Vaglini. Generating images from caption and vice versa via clip-guided generative latent space search. *arXiv preprint arXiv:2102.01645*, 2021. 3
- [13] Ian Goodfellow, Jean Pouget-Abadie, Mehdi Mirza, Bing Xu, David Warde-Farley, Sherjil Ozair, Aaron Courville, and Yoshua Bengio. Generative adversarial networks. *Communications of the ACM*, 63(11):139–144, 2020. 2
- [14] Ian J Goodfellow, Jonathon Shlens, and Christian Szegedy. Explaining and harnessing adversarial examples. *arXiv preprint arXiv:1412.6572*, 2014. 2
- [15] Will Grathwohl, Kuan-Chieh Wang, Jörn-Henrik Jacobsen, David Duvenaud, Mohammad Norouzi, and Kevin Swersky. Your classifier is secretly an energy based model and you should treat it like one. *arXiv preprint arXiv:1912.03263*, 2019. 2, 3
- [16] Kaiming He, Xinlei Chen, Saining Xie, Yanghao Li, Piotr Dollár, and Ross Girshick. Masked autoencoders are scalable vision learners. In *Proceedings of the IEEE/CVF Conference on Computer Vision and Pattern Recognition*, pages 16000–16009, 2022. 4, 11
- [17] Kaiming He, Xiangyu Zhang, Shaoqing Ren, and Jian Sun. Deep residual learning for image recognition. In *Proceedings of the IEEE conference on computer vision and pattern recognition*, pages 770–778, 2016. 2
- [18] Martin Heusel, Hubert Ramsauer, Thomas Unterthiner, Bernhard Nessler, and Sepp Hochreiter. Gans trained by a two time-scale update rule converge to a local nash equilibrium. *Advances in neural information processing systems*, 30, 2017. 5
- [19] Jonathan Ho, Ajay Jain, and Pieter Abbeel. Denoising diffusion probabilistic models. *Advances in Neural Information Processing Systems*, 33:6840–6851, 2020. 2, 3
- [20] Alexia Jolicoeur-Martineau, Rémi Piché-Taillefer, Rémi Taquet des Combes, and Ioannis Mitliagkas. Adversarial score matching and improved sampling for image generation. *arXiv preprint arXiv:2009.05475*, 2020. 3
- [21] Alex Krizhevsky, Ilya Sutskever, and Geoffrey E Hinton. Imagenet classification with deep convolutional neural networks. *Communications of the ACM*, 60(6):84–90, 2017. 2
- [22] Yann LeCun, Léon Bottou, Yoshua Bengio, and Patrick Haffner. Gradient-based learning applied to document recognition. *Proceedings of the IEEE*, 86(11):2278–2324, 1998. 2, 12
- [23] Aravindh Mahendran and Andrea Vedaldi. Understanding deep image representations by inverting them. In *Proceedings of the IEEE conference on computer vision and pattern recognition*, pages 5188–5196, 2015. 2, 3
- [24] Alexander Mordvintsev. Deepdream with tensorflow. 2016. URL: <https://www.tensorflow.org/tutorials/generative/deepdream>, <https://github.com/google/deepdream>. 2, 3, 5, 6, 7, 11, 12
- [25] Alexander Mordvintsev, Christopher Olah, and Mike Tyka. Inceptionism: Going deeper into neural networks. 2015. URL: <https://ai.googleblog.com/2015/06/inceptionism-going-deeper-into-neural.html>. 2, 3
- [26] Charlie Nash, Jacob Menick, Sander Dieleman, and Peter W Battaglia. Generating images with sparse representations. *arXiv preprint arXiv:2103.03841*, 2021. 5
- [27] Anh Nguyen, Jeff Clune, Yoshua Bengio, Alexey Dosovitskiy, and Jason Yosinski. Plug & play generative networks: Conditional iterative generation of images in latent space. In *Proceedings of the IEEE conference on computer vision and pattern recognition*, pages 4467–4477, 2017. 3
- [28] Anh Nguyen, Alexey Dosovitskiy, Jason Yosinski, Thomas Brox, and Jeff Clune. Synthesizing the preferred inputs for neurons in neural networks via deep generator networks. *Advances in neural information processing systems*, 29, 2016. 3
- [29] Anh Nguyen, Jason Yosinski, and Jeff Clune. Deep neural networks are easily fooled: High confidence predictions for unrecognizable images. In *Proceedings of the IEEE conference on computer vision and pattern recognition*, pages 427–436, 2015. 2, 3



- [30] Alexander Quinn Nichol and Prafulla Dhariwal. Improved denoising diffusion probabilistic models. In *International Conference on Machine Learning*, pages 8162–8171. PMLR, 2021. [2](#), [3](#), [5](#)
- [31] Christopher Olah, Ludwig Schubert, Alexander Mordvintsev, Michael Petrov, Jacob Hilton, Badr YOUSSEF IDRISSEI, Abhinav Prakash, Gabriel Goh, Arvind Satyanarayan, Shan Carter, ProGamerGov, Mikael Capelle, Chelsea Sierra Voss, Adam Pearce, Bartosz Miselis, Thomas Tumieli, zan, Teon L Brooks, Mihai Maruseac, Tyler, Samuel Marks, Stefan Sietzen, Nick Cammarata, Marlon, Felix Wege, John Bisognano, Shubhadeep Roychoudhury, Dhruv Guliani, Kevin Mader, Katerina, Kashif Rasul, Rajat gupta, and Nicola Pezzotti. Lucid. 2017. URL: <https://github.com/tensorflow/lucid/>. [2](#), [3](#)
- [32] Aaron van den Oord, Sander Dieleman, Heiga Zen, Karen Simonyan, Oriol Vinyals, Alex Graves, Nal Kalchbrenner, Andrew Senior, and Koray Kavukcuoglu. Wavenet: A generative model for raw audio. *arXiv preprint arXiv:1609.03499*, 2016. [2](#)
- [33] Audun M. Øygaard. Deepdraw. 2015. URL: <https://github.com/auduno/deepdraw>. [2](#), [3](#)
- [34] Audun M. Øygaard. Visualizing googlenet classes. 2015. URL: <https://www.auduno.com/2015/07/29/visualizing-googlenet-classes/>. [2](#), [3](#)
- [35] Or Patashnik, Zongze Wu, Eli Shechtman, Daniel Cohen-Or, and Dani Lischinski. Styleclip: Text-driven manipulation of stylegan imagery. In *Proceedings of the IEEE/CVF International Conference on Computer Vision*, pages 2085–2094, 2021. [3](#)
- [36] Alec Radford, Jong Wook Kim, Chris Hallacy, Aditya Ramesh, Gabriel Goh, Sandhini Agarwal, Girish Sastry, Amanda Askell, Pamela Mishkin, Jack Clark, et al. Learning transferable visual models from natural language supervision. In *International Conference on Machine Learning*, pages 8748–8763. PMLR, 2021. [3](#), [5](#), [9](#), [10](#)
- [37] Aditya Ramesh, Prafulla Dhariwal, Alex Nichol, Casey Chu, and Mark Chen. Hierarchical text-conditional image generation with clip latents. *arXiv preprint arXiv:2204.06125*, 2022. [2](#)
- [38] Aditya Ramesh, Mikhail Pavlov, Gabriel Goh, Scott Gray, Chelsea Voss, Alec Radford, Mark Chen, and Ilya Sutskever. Zero-shot text-to-image generation. In *International Conference on Machine Learning*, pages 8821–8831. PMLR, 2021. [2](#), [9](#), [10](#)
- [39] Ali Razavi, Aaron Van den Oord, and Oriol Vinyals. Generating diverse high-fidelity images with vq-vae-2. *Advances in neural information processing systems*, 32, 2019. [5](#)
- [40] Robin Rombach, Andreas Blattmann, Dominik Lorenz, Patrick Esser, and Björn Ommer. High-resolution image synthesis with latent diffusion models. In *Proceedings of the IEEE/CVF Conference on Computer Vision and Pattern Recognition*, pages 10684–10695, 2022. [2](#)
- [41] Sara Sabour, Nicholas Frosst, and Geoffrey E Hinton. Dynamic routing between capsules. *Advances in neural information processing systems*, 30, 2017. [11](#)
- [42] Chitwan Saharia, William Chan, Saurabh Saxena, Lala Li, Jay Whang, Emily Denton, Seyed Kamyar Seyed Ghasemipour, Burcu Karagol Ayan, S Sara Mahdavi, Rapha Gontijo Lopes, et al. Photorealistic text-to-image diffusion models with deep language understanding. *arXiv preprint arXiv:2205.11487*, 2022. [2](#)
- [43] Chitwan Saharia, Jonathan Ho, William Chan, Tim Salimans, David J Fleet, and Mohammad Norouzi. Image super-resolution via iterative refinement. *IEEE Transactions on Pattern Analysis and Machine Intelligence*, 2022. [3](#), [5](#)
- [44] Tim Salimans, Ian Goodfellow, Wojciech Zaremba, Vicki Cheung, Alec Radford, and Xi Chen. Improved techniques for training gans. *Advances in neural information processing systems*, 29, 2016. [5](#)
- [45] Shibani Santurkar, Andrew Ilyas, Dimitris Tsipras, Logan Engstrom, Brandon Tran, and Aleksander Madry. Image synthesis with a single (robust) classifier. *Advances in Neural Information Processing Systems*, 32, 2019. [2](#), [3](#)
- [46] Karen Simonyan and Andrew Zisserman. Very deep convolutional networks for large-scale image recognition. *arXiv preprint arXiv:1409.1556*, 2014. [2](#)
- [47] Uriel Singer, Adam Polyak, Thomas Hayes, Xi Yin, Jie An, Songyang Zhang, Qiyuan Hu, Harry Yang, Oron Ashual, Oran Gafni, et al. Make-a-video: Text-to-video generation without text-video data. *arXiv preprint arXiv:2209.14792*, 2022. [2](#)
- [48] Jascha Sohl-Dickstein, Eric Weiss, Niru Maheswaranathan, and Surya Ganguli. Deep unsupervised learning using nonequilibrium thermodynamics. In *International Conference on Machine Learning*, pages 2256–2265. PMLR, 2015. [3](#)
- [49] Jiaming Song, Chenlin Meng, and Stefano Ermon. Denoising diffusion implicit models. *arXiv preprint arXiv:2010.02502*, 2020. [3](#)
- [50] Yang Song and Stefano Ermon. Generative modeling by estimating gradients of the data distribution. *Advances in Neural Information Processing Systems*, 32, 2019. [3](#)
- [51] Yang Song, Jascha Sohl-Dickstein, Diederik P Kingma, Abhishek Kumar, Stefano Ermon, and Ben Poole. Score-based generative modeling through stochastic differential equations. *arXiv preprint arXiv:2011.13456*, 2020. [3](#)
- [52] Christian Szegedy, Vincent Vanhoucke, Sergey Ioffe, Jon Shlens, and Zbigniew Wojna. Rethinking the inception architecture for computer vision. In *Proceedings of the IEEE conference on computer vision and pattern recognition*, pages 2818–2826, 2016. [12](#)
- [53] Dimitris Tsipras, Shibani Santurkar, Logan Engstrom, Alexander Turner, and Aleksander Madry. Robustness may be at odds with accuracy. *arXiv preprint arXiv:1805.12152*, 2018. [2](#), [3](#)
- [54] Mike Tyka. Class visualization with bilateral filters. 2016. URL: <https://mtyka.github.io/deepdream/2016/02/05/bilateral-class-vis.html>. [2](#), [3](#)
- [55] Ruben Villegas, Mohammad Babaeizadeh, Pieter-Jan Kindermans, Hernan Moraldo, Han Zhang, Mohammad Taghi Saffar, Santiago Castro, Julius Kunze, and Dumitru Erhan. Phenaki: Variable length video generation from open domain textual description. *arXiv preprint arXiv:2210.02399*, 2022. [2](#)

- [56] Guangrun Wang, Yansong Tang, Liang Lin, and Philip HS Torr. Semantic-aware auto-encoders for self-supervised representation learning. In *Proceedings of the IEEE/CVF Conference on Computer Vision and Pattern Recognition*, pages 9664–9675, 2022. [4](#), [11](#)
- [57] Guangcong Wang, Yinuo Yang, Chen Change Loy, and Ziwei Liu. Stylelight: Hdr panorama generation for lighting estimation and editing. In *European Conference on Computer Vision*, pages 477–492. Springer, 2022. [2](#)
- [58] Jason Yosinski, Jeff Clune, Anh Nguyen, Thomas Fuchs, and Hod Lipson. Understanding neural networks through deep visualization. *arXiv preprint arXiv:1506.06579*, 2015. [3](#)
- [59] Long Zhuo, Guangcong Wang, Shikai Li, Wayne Wu, and Ziwei Liu. Fast-vid2vid: Spatial-temporal compression for video-to-video synthesis. In *European Conference on Computer Vision*, pages 289–305. Springer, 2022. [2](#)

# Supplementary Materials of “Traditional Classification Neural Networks are Good Generators”

Guangrun Wang and Philip H.S. Torr

University of Oxford

{guangrun.wang, philip.torr}@eng.ox.ac.uk

We provide a number of samples generated by CaG in this appendix, and we very much look forward to the readers viewing the images in the appendix below.

## A. Samples of CaG on ImageNet $256 \times 256$

We have provided samples generated by our method in Figure 1 and Figure 4 of the paper. However, the optimization time for each sample needs to be longer, and the number of samples shown needs to be more. Therefore, we present a large number of samples in detail in this supplementary material.

Please feel free to review Figures 10, 11, 12, 13, 5, 14, 6, 15, 16, 17, and 18 below in the Appendix.

## B. Samples of Text-to-Image Generation

In Figure 7 of the article, we show that our method can not only use neural network classifiers for sample generation but, more excitingly, it can also be used for text-to-image generation. We can treat a text-image pre-training model as a generalized classifier and extend CaG to text-to-image generation. In this appendix, we show more examples of text-to-image generation. Please note that we are not chasing high sample quality here, but using fast optimization to get results. We also did not use distance metric loss to increase the diversity of samples.

Please feel free to review Figures 19, 20, 21, and 22 below in the Appendix.





Figure 10. Samples of CaG on ImageNet  $256 \times 256$ . The classes are Class 3 (i.e., tiger shark), Class 5 (i.e., electric ray), Class 8 (i.e., hen), Class 10 (i.e., brambling), and Class 14 (i.e., indigo bunting).





Figure 11. Samples of CaG on ImageNet  $256 \times 256$ . The classes are Class 18 (i.e., magpie), Class 54 (i.e., hognose snake), Class 70 (i.e., harvestman), Class 71 (i.e., scorpion), and Class 79 (i.e., centipede).



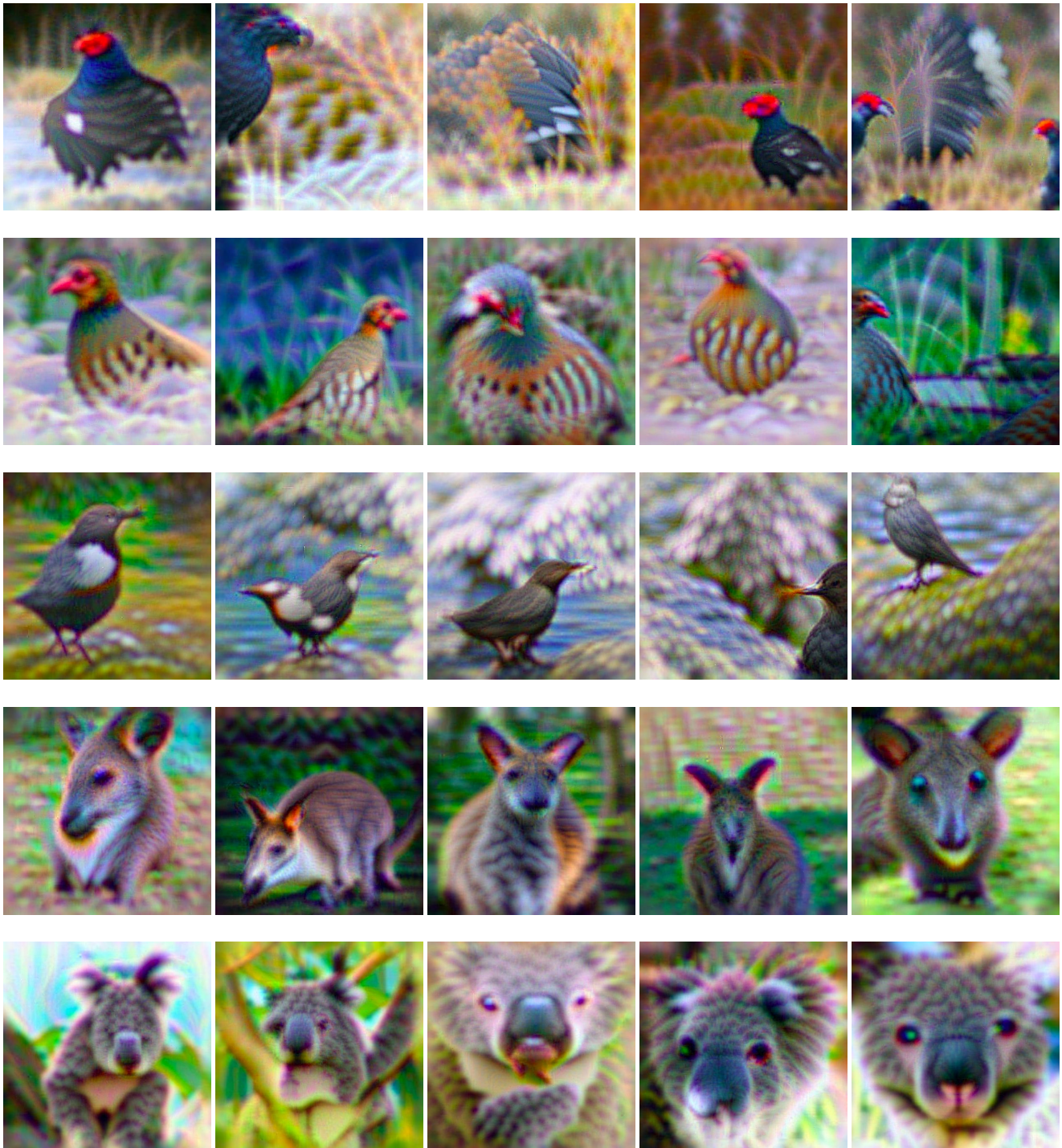


Figure 12. Samples of CaG on ImageNet  $256 \times 256$ . The classes are Class 80 (i.e., black grouse), Class 86 (i.e., partridge), Class 20 (i.e., water ouzel), Class 104 (i.e., wallaby), and Class 105 (i.e., koala).





Figure 13. Samples of CaG on ImageNet  $256 \times 256$ . The classes are Class 106 (i.e., wombat), Class 107 (i.e., jellyfish), Class 107 (i.e., jellyfish), Class 108 (i.e., sea anemone), and Class 110 (i.e., flatworm).





Figure 14. Samples of CaG on ImageNet  $256 \times 256$ . The classes are Class 117 (i.e., chambered nautilus), Class 118 (i.e., Dungeness crab), Class 120 (i.e., fiddler crab), Class 121 (i.e., king crab), and Class 125 (i.e., hermit crab).



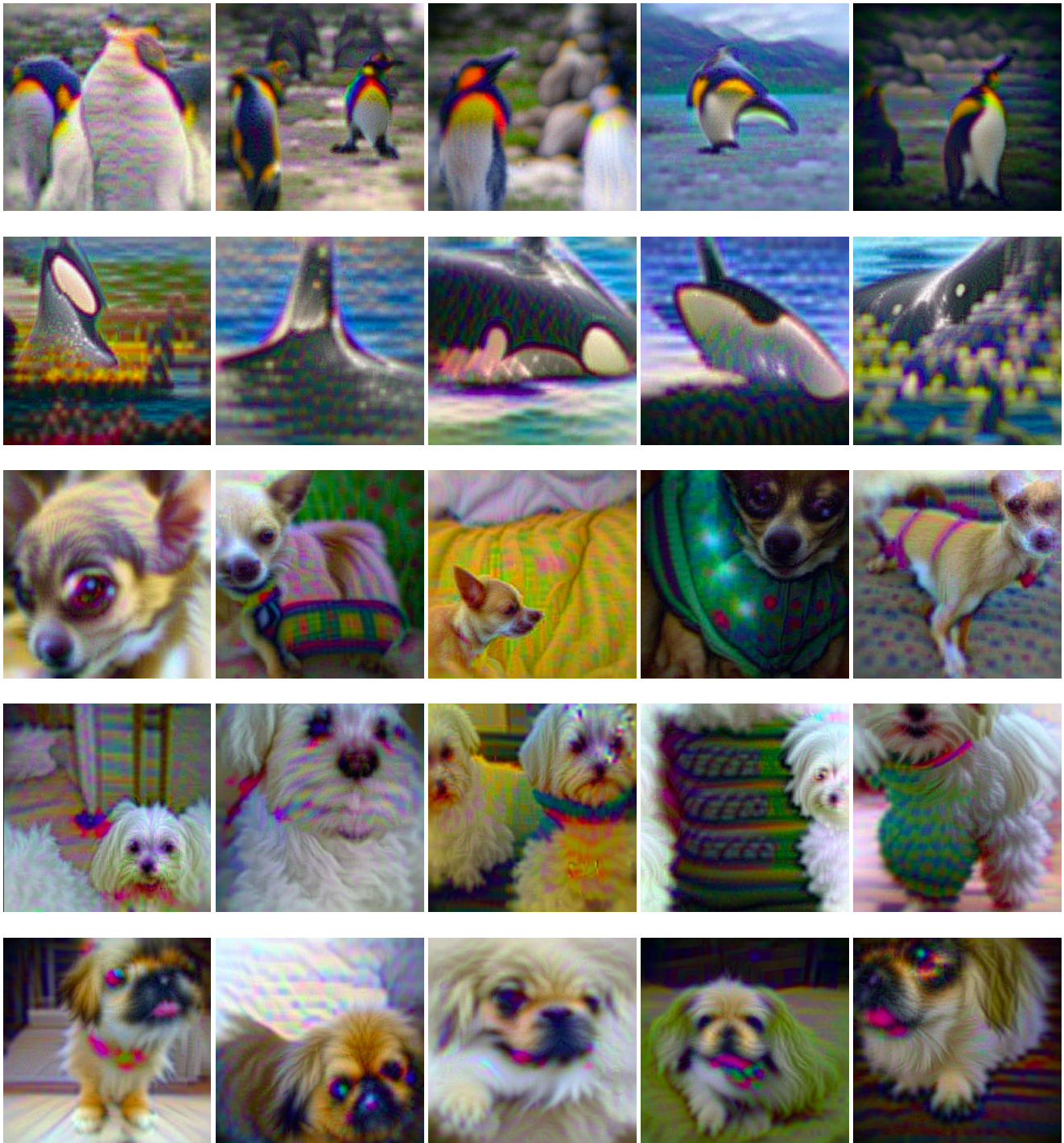


Figure 15. Samples of CaG on ImageNet  $256 \times 256$ . The classes are Class 145 (i.e., king penguin), Class 148 (i.e., killer whale), Class 151 (i.e., Chihuahua), Class 153 (i.e., Maltese dog), and Class 154 (i.e., Pekinese).



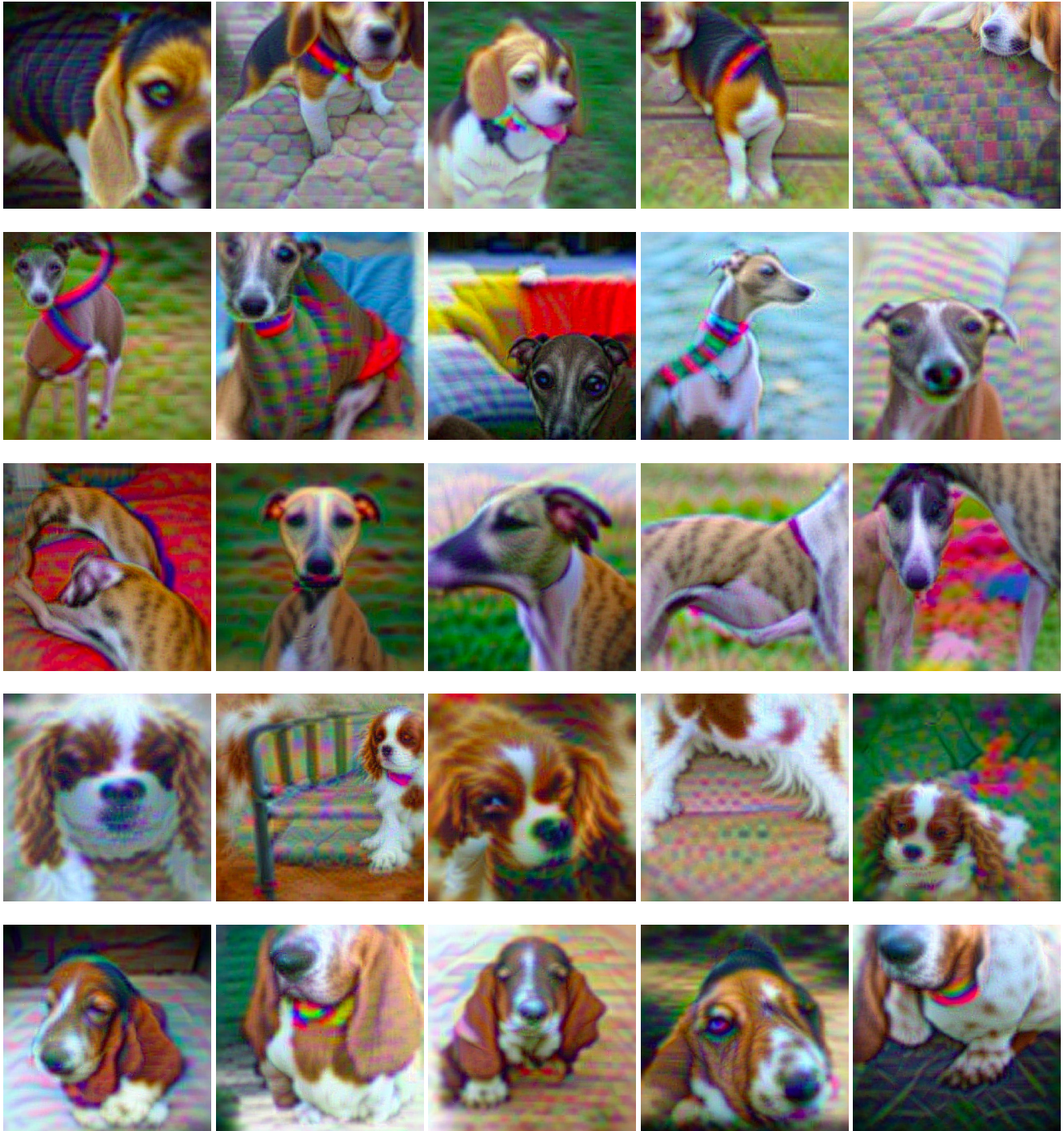


Figure 16. Samples of CaG on ImageNet  $256 \times 256$ . The classes are Class 162 (i.e., beagle), Class 171 (i.e., Italian greyhound), Class 172 (i.e., whippet), Class 156 (i.e., Blenheim spaniel), and Class 161 (i.e., basset).



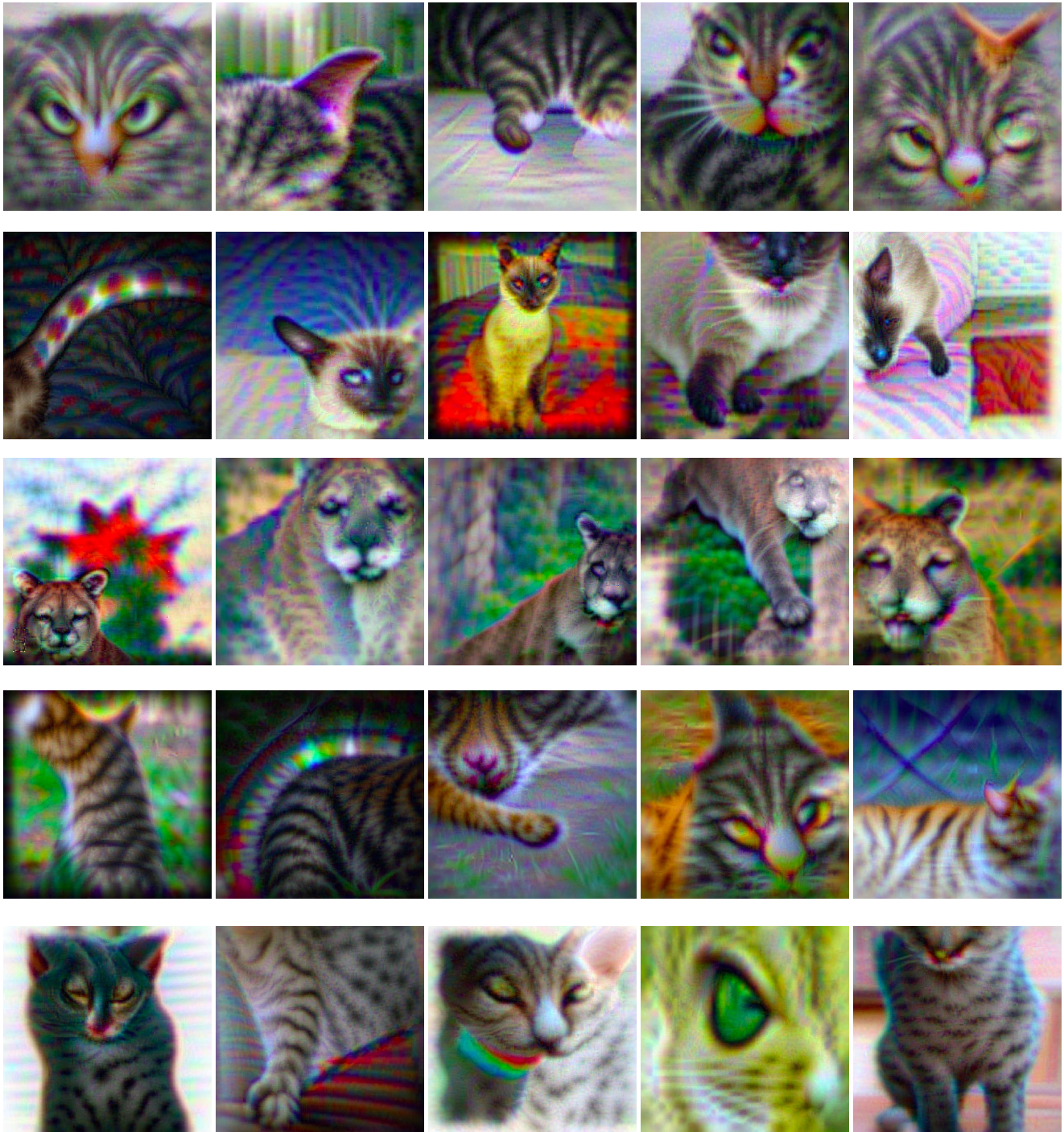


Figure 17. Samples of CaG on ImageNet  $256 \times 256$ . The classes are Class 281 (i.e., tabby cat), Class 284 (i.e., Siamese cat), Class 286 (i.e., cougar), Class 282 (i.e., tiger cat), and Class 285 (i.e., Egyptian cat).





Figure 18. Samples of CaG on ImageNet  $256 \times 256$ . The classes are Class 423 (i.e., barber chair), Class 423 (i.e., barber chair), Class 765 (i.e., rocking chair), Class 559 (i.e., folding chair), and Class 831 (i.e., studio couch).





“an illustration of a baby daikon radish in a tutu walking a dog”

Figure 19. Text-to-image generation using a pretrained text-image model CLIP. Note that we are not chasing high sample quality here, but using fast optimization to get results. We also did not use distance metric loss to increase the diversity of samples.





“an armchair in the shape of an avocado”

Figure 20. Text-to-image generation using a pretrained text-image model CLIP. Note that we are not chasing high sample quality here, but using fast optimization to get results. We also did not use distance metric loss to increase the diversity of samples.





“a photo of a phone from the 20s”

Figure 21. Text-to-image generation using a pretrained text-image model CLIP. Note that we are not chasing high sample quality here, but using fast optimization to get results. We also did not use distance metric loss to increase the diversity of samples.





“An astronaut playing basketball with cats in space as a children book illustration”

Figure 22. Text-to-image generation using a pretrained text-image model CLIP. Note that we are not chasing high sample quality here, but using fast optimization to get results. We also did not use distance metric loss to increase the diversity of samples.